

See discussions, stats, and author profiles for this publication at: <https://www.researchgate.net/publication/317606079>

Divide-and-Allocate: An Uplink Successive Bandwidth Division NOMA System

Article in Transactions on Emerging Telecommunications Technologies · September 2017

DOI: 10.1002/ett.3216

CITATIONS

27

READS

668

3 authors:



Soma Qureshi

University of Engineering and Technology, Taxila

4 PUBLICATIONS 47 CITATIONS

[SEE PROFILE](#)



Syed Ali Hassan

National University of Sciences & Technology

236 PUBLICATIONS 2,270 CITATIONS

[SEE PROFILE](#)



Dush Nalin K Jayakody

Tomsk Polytechnic University

211 PUBLICATIONS 2,058 CITATIONS

[SEE PROFILE](#)

Some of the authors of this publication are also working on these related projects:



mmWave for access and back-haul in future generation networks. [View project](#)



UAV-aided Wireless Communication [View project](#)

RESEARCH ARTICLE

Divide-and-Allocate: An Uplink Successive Bandwidth Division NOMA System

Soma Qureshi^{1*} Syed Ali Hassan¹ and Dushantha Nalin K. Jayakody²

¹ School of Electrical Engineering & Computer Science (SEECS), National University of Sciences & Technology (NUST), Islamabad, Pakistan. E-mail: {14mseesqureshi, ali.hassan}@seecs.edu.pk

² Department of Software Engineering, Institute of Cybernetics National Research Tomsk Polytechnic University, Russia. E-mail: nalin@tpu.ru

ABSTRACT

This paper investigates a new spectrum sharing strategy using non-orthogonal multiple access (NOMA), a technique that is expected to lead towards the fifth generation (5G) of wireless networks. The proposed scheme, successive bandwidth division (SBD)-NOMA, is a hybrid approach exploiting characteristics of both the conventional NOMA system and the orthogonal multiple access (OMA) system. Power allocation is being performed in SBD-NOMA to maximize the sum rate using a divide-and-allocate approach such that all users are allocated with an optimal transmission power. Under Rayleigh fading, the probability density function (PDF) of the received signal-to-interference plus noise ratio (SINR) is derived and closed-form expressions for the outage probability are presented when channel state information (CSI) is available at the base station (BS). The performance evaluation is carried out in terms of receiver complexity, average sum rate and outage probability. Simulations results are provided to access and compare the performance of the proposed scheme with other contemporary approaches. Copyright © 2016 John Wiley & Sons, Ltd.

*Correspondence

School of Electrical Engineering & Computer Science (SEECS), National University of Sciences & Technology (NUST), Islamabad, Pakistan. E-mail: 14mseesqureshi@seecs.edu.pk

1. INTRODUCTION

RECENTLY, many research studies focus on designing future mobile networks, which are capable of supporting the overwhelming demand for data traffic in 2020 and beyond. One of the challenges to meet the future traffic demand is to provide high spectral efficiency, which is possible by efficient design of multiple access schemes in future cellular networks in addition to other technologies. The demand to design the next generation wireless networks has long been sought. Several metrics and parameters have been considered as performance measures, e.g., spectral efficiency, reliability, quality of service (QoS),

efficient utilization of radio resources and energy efficiency etc. Researchers from both industry and academia are exploring the domains of a multitude of techniques for future networks including device-to-device (D2D) communication, ultradensification, millimeter wave (mmWave) communication, massive multiple-input multiple-output (MIMO) and novel multiple access schemes under the umbrella of fifth generation (5G) networks [1, 2].

The design of an appropriate multiple access method is one of the most significant challenge in optimizing the system capacity. The multiple access methods can be sketchily branded into two main methods; orthogonal multiple access (OMA) and non-orthogonal multiple access (NOMA) [3]. An orthogonal scheme permits

a seamless receiver to completely separate unsolicited signals from the desired signal using different basis functions, i.e., signals from separate users are orthogonal to one another in orthogonal schemes. Time division multiple access (TDMA) and orthogonal frequency-division multiple access (OFDMA) are the examples of OMA schemes.

NOMA, on the other hand, is considered as a candidate multiple access scheme for 5G wireless networks because of its ability to share space resource among multiple users in addition to other benefits being offered. By virtue of this property, NOMA provides higher spectral efficiency, reduced latency, massive connectivity, ultra-fast speeds and user fairness [4] as compared to the traditional multiple access techniques. The key feature of NOMA is to explore the multiplexing gain in power domain. NOMA superimposes user signals on top of one another at the transmitter and uses successive interference cancellation (SIC) at the receivers, thus accommodating a large number of users via non-orthogonal resource sharing. Contrary to the conventional water-filling power allocation strategy, NOMA technique allocates more transmit power to the users with poor channel conditions (i.e., weak users) and less transmit power to the users with better channel conditions (i.e., strong users) to set power difference between the users that allows postcoding to suppress or minimize the interference and exploits the gain from NOMA within users. In this case, the weak users can decode their high powered signals directly by treating other signals as noise. In contrast, those users with better channel conditions (i.e., strong users) adopt the SIC technique for signal detection. In this way, the low powered signals are recovered after SIC [5]. It has been demonstrated that by using superposition coding (SC) together with SIC, both the system throughput and user fairness are significantly improved in NOMA systems compared to conventional OMA systems.

1.1. Literature and Motivation

The concept of NOMA is not new as it can be linked to many well-known methods used in previous communication systems. Early works on NOMA system generally consider a transmitter with single antenna. However, it can also be extended to various systems. *Ding et al.* study the ergodic sum rate and outage performance of downlink (DL) NOMA with randomly

deployed single antenna nodes in [6]. Other work on resource allocation in DL NOMA has been characterized in [7]. Recently, some attempts are made to combine NOMA with MIMO to achieve high spectral efficiency as the application of MIMO to NOMA provides additional degrees of freedom [5]. However, the scheme proposed in [5] does not need channel state information (CSI) at the transmitter, rather it requires the larger number of receive antennas as compared to the transmitter. Most of existing work on MIMO-NOMA, such as [8] and [9], has assumed perfect knowledge of CSI at the transmitter, which is difficult to realize in practice. The perfect CSI assumption can consume high bandwidth particularly in massive MIMO scenarios [10]. In [11], the author proposes random opportunistic beamforming for the MIMO NOMA systems, where the base station (BS) transmitter generates multiple beams and superimposes multiple users within each beam. A massive MIMO-NOMA downlink transmission protocol is proposed recently, which does not require the users to feed their channel matrices back to the BS. Some other works include [12] and [13]. Various algorithmic frameworks for optimizing the design of beamforming in the NOMA transmission system have been considered in [14]. In [15] an optimization problem is formulated for various MIMO NOMA scenarios. A signal alignment based precoding scheme was developed in [16], which requires fewer antennas at the users compared to the scheme proposed earlier in [5]. Power allocation between two users is carried out for open-loop MIMO downlink transmissions (i.e., the BS allocates the power to two users signals based on statistical CSI. In [17], a zero-forcing (ZF)-based beamforming and user pairing scheme is proposed for the DL multiuser NOMA system, assuming perfect CSI at the transmitter. More details on MIMO NOMA can be found at [18]. Both the papers [19], [20] have also worked on the downlink scenario. The number of the candidate users in the above paper is not more than N_{max} , which is fixed to 2 in that proposed paper. Similarly, [19] also solved the power allocation problem for a DL scenario as a many-to-many matching game with externalities and a geometric programming, which is one of the efficient method to solve the resource allocation problem, the other being optimization theory and the coalition formation games. An uplink (UL) NOMA transmission scheme is proposed in [21]. Similarly, in [22], the impact of user

pairing is characterized by analyzing the sum rates in two NOMA systems. Some other existing work, for e.g., [23], [24], [25] and [26] on the design of UL NOMA for 5G wireless network has been proposed. Recent works on uplink NOMA are considered in [27] and [28]. An uplink power back-off policy was proposed to distinguish users in a NOMA cluster with nearly similar signal strengths (given that traditional uplink power control is applied). Closed-form analysis was performed for ergodic sum-rate and outage probability of a two-user NOMA cluster. Further, the problem of user scheduling in uplink NOMA has been investigated by various researchers in [29]. However, the performance gain of [29] is limited due to the use of naive power control schemes such as fixed power allocation (FPA) and FTPC for multiplexed users. A joint subcarrier allocation and power control in uplink NOMA is investigated in [30] with perfect SIC at the BS, which is proved to be NP-hard and solved by a near-optimal solution based on Lagrangian duality and dynamic programming (LDA). A game theoretic algorithm for uplink power control has been designed in [31] considering a two-cell NOMA system, where inter-cell interference is assumed to be Gaussian distributed. However, most of the previous works on MC-NOMA considers only two user scenario such as in [31] and [32]. The proposed scheme also offers high computational complexity as compared to our work. Other work on multi-carrier NOMA is considered in [33]. In conventional multicarrier systems, a given radio frequency band is divided into multiple orthogonal subcarriers and each subcarrier is allocated to at most one user to avoid multiuser interference (MUI). The spectral efficiency of such systems can be improved significantly by performing the joint user scheduling and power allocation. In fact, spectral efficiency can be further improved by applying NOMA in multicarrier systems by exploiting the degrees of freedom offered by multiuser diversity and the power domain simultaneously. In [4], the authors demonstrated that MC-NOMA systems employing a suboptimal power allocation scheme achieve system throughput gains over conventional MC-OMA systems. The authors of [34] proposed a suboptimal joint power and subcarrier allocation algorithm for MC-NOMA systems. Yet, the resource allocation schemes proposed in [4], [34] are strictly suboptimal. Some other significant works include the combination of NOMA with cooperative communications and mmWave, which has

been characterized in [35, 36]. System level performance of an OFDMA-based NOMA system with fractional transmit power allocation (FTPA) and equal transmit power allocation (ETPA) is considered in [37]. Some other work on power allocation has been discussed in [38, 39]. In [40], the author has presented different power allocation schemes for NOMA considering FTPA, full search power allocation (FSPA) and fixed power allocation (FPA). The FSPA performs well but it has high computational complexity. FPA has worse performance but least complexity. FTPA is a balance between the two but it does not distribute power among the multiplexed users in an optimum way to maximize sum rate. Similarly, in these existing works, the maximum achievable improvement in spectral efficiency of optimal MC-NOMA systems compared to MC-OMA systems is also still unknown. Therefore, for an UL OFDMA-based NOMA system, we have proposed a hybrid multiple access scheme. Compared to these existing works, the motivation of this paper is as follows:

In conventional OMA schemes, multiple users are allocated with radio resources that are orthogonal in time, frequency, or code domain. Ideally, no interference arises due to orthogonal resource allocation, hence, simple single-user detection can be used to separate different users signals. NOMA, on the other hand, allows controllable interference by non-orthogonal resource allocation at the expense of enhanced receiver complexity. In NOMA, all the users can use resources simultaneously, which leads to interuser interference. Hence, more complicated multi-user detection (MUD) techniques are required to retrieve the users signals at the receiver. The optimal approach for uplink NOMA is to allow all the users to share each resource element, and the users power allocated through iterative water-filling [41]. However, in the optimal (unconstrained) NOMA scheme, there is no control over the number of users that share each subcarrier, which makes the MUD at the receiver infeasible. This problem can be mitigated by imposing an upper-limit on the number of users per resource to reduce the receiver complexity. In order to further reduce the interference, we have also divided the available bandwidth into identical orthogonal groups. The proposed scheme not only reduces the number of MUD but also offers reduce complexity and interference. It also eliminates the need of complex receiver designing, which reduces the

cost and also provide enhanced quality-of-service (QoS). Hence, situations where user priority is reduced cost and enhanced QoS, SBD-NOMA schemes should be preferred over conventional UL NOMA that provide better rate and a fairly reliable transmission scheme. Therefore, in order to manage the inter-set interference efficiently, for the UL of an OFDMA-based NOMA system, we propose a suboptimal algorithm known as successive bandwidth division (SBD)-NOMA. As the proposed scheme involve a hybrid multiple access scheme SBD-NOMA, consisting of both orthogonal and non-orthogonal transmissions, therefore, it inherits the advantages of both techniques. In the proposed scheme, the total number of users are orthogonally divided into different sub-bands on the basis of their channel state information (CSI) with limited number of users in each sub-band. Depending upon the number of users in each sub-band, the total bandwidth is divided into orthogonal groups. "Hence, the SBD scheme divides the available bandwidth W , of K users, into K/P identical orthogonal sub-bands, each having a bandwidth of W_{sb} , where P is the number of users in each sub-band. Hence, the successive addition of users in the system divides the bandwidth successively into orthogonal bands". Because of the orthogonality among the group of users, no joint processing is required at the receiver side to retrieve the users signals. As the proposed scheme captured the aforementioned properties we name it SBD-NOMA scheme. To illustrate the concept further. Please see Fig.1. In this Figure the users are occupying the whole available bandwidth in case of NOMA system. It accommodates all users in the same frequency band. This is not the case with OMA. In OMA all the users have separate identical orthogonal sub-bands. The bandwidth available to each user reduces by a factor of $1/K$. There is a single user in each sub-band and the resource block allocated are completely orthogonal. For SBD-NOMA, the users are divided into identical orthogonal sub-bands. However, there does not exist a single user for single sub-band. The number of users in each sub-band is P . The total number of sub-bands is $K = P$. For $P = 2$, the SBD NOMA specializes to NOMA₂, for $P = 4$ the SBD-NOMA specializes to NOMA₄. Similarly, for $P = 8$ the SBD-NOMA specializes to NOMA₈. In order to further reduce the inter-set interference, the users within the same sub-band are paired. The users paired within the same sub-band are members of two distinct sets, namely

strong set and weak set. The sets are classified on the basis of the channel conditions. The members of weak set should be chosen in a way that they offer very little or no interference to the other users within the same sub-band. As the proposed system is formed by combining OMA and NOMA techniques, it inherits the advantages of both techniques. However, grouping cannot exploit the full potential of NOMA and for that, we perform optimal power allocations. In this paper, we mainly focus on the power allocation for MIMO-NOMA when CSI is available at the BS. The main contribution of this paper are as follows:

- We first consider an OFDMA-based MIMO-NOMA UL scenario, known as SBD-NOMA, with a fixed set of power allocation coefficients. There are many differences between an uplink and a downlink NOMA system in terms of implementational complexity, intra cell/ intra cluster interference, SIC at the receiver etc., which can be found in [42]. The performance of this proposed SBD-NOMA is characterized with conventional OMA by using the criteria of sum capacity and outage probability.
- An approach to perform the optimal power allocation coefficients for SBD-NOMA with transmission power constraint is proposed. This is because the choice of the power allocation coefficients is a key to achieve a favorable throughput-fairness tradeoff in NOMA systems. Analytical results, such as an exact expressions of power allocation coefficients, are derived for a two user scenario under a total power constraint.
- Under Rayleigh fading, the probability density function (PDF) of the received signal-to-interference plus noise ratio (SINR) is approximated by a gamma distribution and closed-form expressions for the outage probability are presented for SBD-NOMA with no intra-set interference.

1.2. Organization

The paper is organized as follows. Section 2 presents the system model of UL SBD-NOMA scheme with multiple antennas along with the algorithm for strong and weak set formation and subchannel allocation. Section 3 formulates the sum rate maximization problem and discusses the

optimal solutions for two user scenario. Closed-form expressions of outage probability are derived in Section 4. Simulation results and discussion are provided in Section 5. The paper is concluded with some remarks in Section 6.

1.3. Notation

Matrices and vectors are denoted by upper and lower-case boldface letters, respectively. The superscripts $(\cdot)^T$, $(\cdot)^{-1}$ and $(\cdot)^*$ denote the transpose, inverse and complex conjugate, respectively. For a matrix H , $h_{i,m}$ represents the $(i,m)^{th}$ element of H . The $\mathcal{CN}(0,1)$ represents the distribution of circularly symmetric complex Gaussian (CSCG) random vector with zero mean and unit variance.

2. SYSTEM MODEL

This paper considers an UL multi-user (MU) MIMO scenario, where a BS, equipped with N antennas, communicates with K single antenna users, where $K \geq 2N$. The transmission occurs in the presence of additive white Gaussian noise (AWGN) over Rayleigh flat fading channels with path loss. In schemes other than NOMA, like a conventional UL system with N BS antennas, only N users can be supported at any instance without interference. The novelty of the proposed UL scheme is that, the BS can support $2N$ randomly deployed users at any given instance by SC. In this paper, the term ‘set’ refers to N randomly deployed users chosen on the basis of the channel gains. The sets are classified as *strong* if the corresponding channel gains are large and *weak* if the corresponding channel gains are small, respectively. The sets are determined by sorting the channel gains in descending order and then dividing the channel gains into two halves. The sets thus formed are assumed to be mutually exclusive.

The OMA scheme divides the entire available spectrum into K sub-bands and all K users can be supported simultaneously without any interference. However, the bandwidth available to each user reduces by a factor of $1/K$ for the sake of ensuring orthogonality. For the proposed NOMA system, the users are squashed in the same frequency band. As NOMA accommodates all users in the same frequency band, the interference among users is quite high. Therefore, in order to efficiently manage

the intra-set interference in NOMA assisted networks, the proposed technique works as follows.

2.1. Proposed SBD Scheme

The SBD scheme divides the available bandwidth W , of K users, into K/P identical orthogonal sub-bands, each having a bandwidth of W_{sb} . Here P denotes the maximum number of users that can share a sub-band, where $\{P \in \mathbb{N} \mid 1 \leq P \leq K\}$ and \mathbb{N} is a set of natural numbers. The number P leads to the formation of sub-bands with different bandwidths, depending on its value. The superposition of relatively small number of users in each sub-band reduces the receiver complexity and simple user detection techniques can be applied at the receiver side. The P users paired within the same sub-band are chosen from two mutually exclusive sets A and B whose channel coefficients are pairwise orthogonal.

To get some more insight, consider Fig. 1, where the concept of SBD-NOMA is demonstrated. Let the total number of users $K = 24$. For subsequent discussion in this paper, we define a set ϕ , which is the set of the factors of K . For $K = 24$, $\phi = \{1, 2, 3, 4, 6, 8, 12, 24\}$. Since, the users paired within each sub-bands are assumed to be equal, hence all even elements from ϕ are chosen. Note that when $P = 1$, conventional OMA scheme works for each sub-band and when $P = K$, the SBD scheme specializes to conventional NOMA. For $P = 2$, the access scheme is denoted as NOMA₂, where the number of users in each sub-band is 2 while the total sub-bands are 12. The number P further divides the strong and weak sets A and B into K/P smaller sets such that $\sum_{m=1}^{K/P} A_m \cup B_m = \xi$, where ξ is a set of all K users and m being the sub-band index. Each A_m and B_m from the sets A and B has a cardinality of 1 for $P = 2$ while there is a single interferer in this case. Similarly, for $P = 4$, SBD-NOMA has 4 users in each sub-band. Each A_m and B_m from the sets A and B has cardinality of 2, whereas the number of interferers is 3 in this case. $P = K$ specializes to the case of conventional UL NOMA, with only one sub-band and $(K - 1)$ interferers. In other words, we define NOMA _{P} to be the access scheme where K/P sub-bands are formed with P users in each sub-band and a conventional NOMA scheme works in each of sub-band.

The number P will affect the number of sub-bands, interferers, dimensions of channel and detection matrices, dimensions of received signal and the number of users in

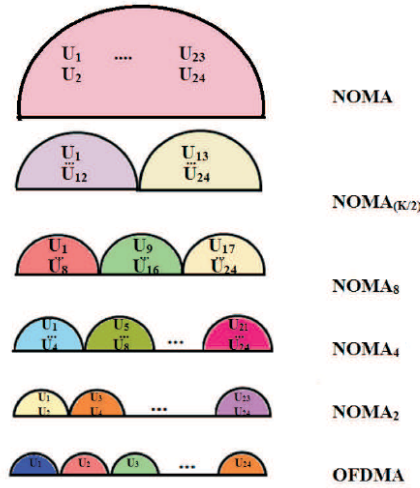


Figure 1. OFDMA vs. NOMA and proposed SBD scheme, $K=24$ for this particular example.

each sub-band. However, the total number of users remains the same. As only P users can transmit their signals at any given instance, hence the received signal is the superposition of the signals from P users. The remaining users are orthogonal. Therefore, in the proposed UL SBD scheme, the decoding complexity is $O(|\chi|^P)$, while that of conventional NOMA with K users is $O(|\chi|^K)$, where χ denotes the constellation alphabet. **This is the worst case complexity. For higher order modulation schemes, we have other more efficient and reduced complexity algorithms like sphere decoding. There is also an option to use parallel processing for higher order modulation decoding.** However, dividing the entire bandwidth into sub-bands cannot exploit the full potential of NOMA, where all users can occupy the entire bandwidth. Therefore, to cope with this we perform optimal power allocation in SBD-NOMA, which provides an achievable rate much better than the one achieved by without power allocation.

2.2. Received Signal Model for proposed UL SBD-NOMA

Let's denote the channel matrices of strong and weak sets as \mathbf{H}_1 and \mathbf{H}_2 , respectively, written as

$$\mathbf{H}_1 = \begin{bmatrix} \mathbf{h}_{1,1} & \mathbf{h}_{1,2} & \dots & \mathbf{h}_{1,P/2} \end{bmatrix}, \quad (1)$$

$$\mathbf{H}_2 = \begin{bmatrix} \mathbf{h}_{2,1} & \mathbf{h}_{2,2} & \dots & \mathbf{h}_{2,P/2} \end{bmatrix}, \quad (2)$$

where $\mathbf{h}_{1,j}$ and $\mathbf{h}_{2,n}$ denote the $(N \times 1)$ UL channel vectors of the j^{th} strong and n^{th} weak user, respectively, and are drawn from the complex Gaussian distribution with zero mean and unit variance. The channel vectors are Rayleigh flat faded with path loss. Thus, in the given scenario, the superimposed signal received by the entire group of P users, multiplexed on the m^{th} sub-band, where $1 \leq m \leq K/P$, is given by

$$\mathbf{y} = (\mathbf{H}_1 \mathbf{s}_1 + \mathbf{H}_2 \mathbf{s}_2) + \mathbf{n}, \quad (3)$$

where \mathbf{y} is an $(N \times 1)$ UL received signal vectors, $\mathbf{s}_1 = [\sqrt{\alpha_{1,1}}x_{1,1} \dots \sqrt{\alpha_{1,P/2}}x_{1,P/2}]^T$ and $\mathbf{s}_2 = [\sqrt{\alpha_{2,1}}x_{2,1} \dots \sqrt{\alpha_{2,P/2}}x_{2,P/2}]^T$ are $(P/2 \times 1)$ signal vectors of strong and weak sets, respectively. Here, $(\cdot)^T$ denotes the transpose, $\alpha_{i,j}$ represents the NOMA power allocation coefficient of strong and weak users and $x_{i,j}$ represents the symbol transmitted by the j^{th} user to the BS with N antennas and i represents being a member of strong or weak set. The \mathbf{n} is an $(N \times 1)$ AWGN vector, where each value is a normal random variable with zero mean and unit variance. The total number of signals received by the BS is K/P and it depends on the number of users within a particular sub-band.

The received signal of an n^{th} strong user, chosen from the set J , where $J = \{1, 2, \dots, P/2\}$ and $n \in J$ is the superimposed signal given by

$$\mathbf{y}_n = \mathbf{h}_{1,n} \sqrt{\alpha_{1,n}} x_{1,n} + \sum_{j=1}^{P/2} \mathbf{h}_{2,j} \sqrt{\alpha_{2,j}} x_{2,j} + \mathbf{n}, \quad (4)$$

where $\mathbf{h}_{1,n}$ and $\mathbf{h}_{2,n}$ are the $(N \times 1)$ UL channel vectors of the n^{th} user from both strong and weak sets to the BS having N antennas and \mathbf{n} is the $(N \times 1)$ AWGN vector.

Since the BS receives superimposed signals, an SIC scheme is required at the receiver side for decoding, the signals of the strong set are decoded first, with interference from weak set, while the users in the weak set are free from inter-set interference. The remaining users are orthogonal and offer no inter-set interference.

As this paper assumes perfect CSI, a ZF postcoded or detection matrix is used to decode the signals of strong and weak sets. The corresponding postcoding matrix \mathbf{Z}_i

is given by

$$\mathbf{Z}_i = [\mathbf{z}_{i,1}^\top \quad \mathbf{z}_{i,2}^\top \quad \cdots \quad \mathbf{z}_{i,P/2}^\top]^\top = (\mathbf{H}_i)^* ((\mathbf{H}_i)(\mathbf{H}_i)^*)^{-1}. \quad (5)$$

In the above equation, \mathbf{Z}_1 is the $(P/2 \times N)$ postcoded matrix of users in the strong set and $\mathbf{z}_{i,j}$ is the $(1 \times N)$ vector corresponding to the ZF UL channel vector of the j^{th} user, respectively. The application of postcoded ZF matrix at the receiver forms N decoupled data substreams, which makes the system MIMO NOMA rather than MISO NOMA.

2.3. Received SINR

In order to determine the SINR of strong and weak users, respectively, we apply the postcoded matrix \mathbf{Z}_1 to decode the users of strong set, where the received signal vector $\mathbf{r}^{(1)} = [r_{1,1}, r_{1,2}, \dots, r_{1,P/2}]$ becomes

$$\mathbf{r}^{(1)} = \mathbf{Z}_1 \mathbf{y} = \mathbf{Z}_1 \mathbf{H}_1 \mathbf{s}_1 + \mathbf{Z}_1 \mathbf{H}_2 \mathbf{s}_2 + \mathbf{Z}_1 \mathbf{n}, \quad (6)$$

where $\mathbf{r}^{(1)}$ is an $(N/(K/P) \times 1)$ received signal vector. From (6), the signal of the n^{th} user in the strong set, chosen from the set J , where $n \in J$ is as follow

$$r_{1,n}^{(1)} = \mathbf{z}_{1,n} \mathbf{h}_{1,n} \sqrt{\alpha_{1,n}} x_{1,n} + \sum_{j=1}^{P/2} \mathbf{z}_{1,n} \mathbf{h}_{2,j} \sqrt{\alpha_{2,j}} x_{2,j} + \mathbf{z}_{1,n} \mathbf{n}. \quad (7)$$

The corresponding SINR of an n^{th} strong user is given by

$$SINR_{1,n} = \frac{|\mathbf{h}_{1,n} \cdot \mathbf{z}_{1,n}|^2 \alpha_{1,n}}{\sum_{j=1}^{P/2} |\mathbf{h}_{2,j} \cdot \mathbf{z}_{1,n}|^2 \alpha_{2,j} + \sigma_n^2}, \quad (8)$$

where $|\cdot|$ denotes the norm operator and $(\mathbf{a} \cdot \mathbf{b})$ represents the point to point multiplication between any two vectors \mathbf{a} and \mathbf{b} . The $|\mathbf{h}_{1,n} \cdot \mathbf{z}_{1,n}|^2 \alpha_{1,n}$ represents the desired signal of n^{th} strong user from the set J while the signal $\sum_{j=1}^{P/2} |\mathbf{h}_{2,j} \cdot \mathbf{z}_{1,n}|^2 \alpha_{2,j}$ represents the inter-set interference from weak users. The users are experiencing the intra-set interference. The strong and weak users will encounter interference from other strong and weak users, respectively. However, by choosing the transmit antennas more than or equal to receive antennas, the postcoded ZF matrix formed at the receiver are perfectly square, which automatically eliminates the interference from other strong and weak users within the same set. In this case, each

channel vector and the ZF postcoding vector satisfies the following condition:

$$\mathbf{z}_{1,j} \cdot \mathbf{h}_{1,n} = 0; \forall j \neq n, j \in \{1, 2, \dots, P/2\}. \quad (9)$$

However, when the BS is equipped with less than N antennas, then the resultant matrix becomes rectangular. Thus, the strong and weak users also encounter the interference from other strong and weak users, respectively. Consequently, the strong set is affected by a total interference of I , which can be expanded as,

$$I = \sum_{j=1, j \neq n}^{P/2} |\mathbf{h}_{1,j} \cdot \mathbf{z}_{1,n}|^2 \alpha_{1,j} + \sum_{j=1}^{P/2} |\mathbf{h}_{2,j} \cdot \mathbf{z}_{1,n}|^2 \alpha_{2,j}, \quad (10)$$

and the corresponding SINR becomes,

$$SINR_{1,n} = \frac{|\mathbf{h}_{1,n} \cdot \mathbf{z}_{1,n}|^2 \alpha_{1,n}}{I + \sigma_n^2}, \quad (11)$$

where $\sum_{j=1, j \neq n}^{P/2} |\mathbf{h}_{1,j} \cdot \mathbf{z}_{1,n}|^2 \alpha_{1,j}$ represents the intra-set interference from the other strong users, respectively.

For decoding of weak user signal, SIC is carried out so there will be no interference in this case. Hence, after applying ZF matrix, the signals of weak set become

$$\mathbf{r}^{(2)} = \mathbf{Z}_2 \mathbf{H}_2 \mathbf{s}_2 + \mathbf{Z}_2 \mathbf{n}, \quad (12)$$

The received signal and corresponding SINR of n^{th} weak user chosen from the set J , becomes

$$r_{2,n}^{(2)} = \mathbf{z}_{2,n} \mathbf{h}_{2,n} \sqrt{\alpha_{2,n}} x_{2,n} + \mathbf{z}_{2,n} \mathbf{n}, \quad (13)$$

$$SINR_{2,n} = \frac{|\mathbf{h}_{2,n} \cdot \mathbf{z}_{2,n}|^2 \alpha_{2,n}}{\sigma_n^2}. \quad (14)$$

In case of intra-set interference,

$$SINR_{2,n} = \frac{|\mathbf{h}_{2,n} \cdot \mathbf{z}_{2,n}|^2 \alpha_{2,n}}{\sum_{j=1, j \neq n}^{P/2} |\mathbf{h}_{2,j} \cdot \mathbf{z}_{2,n}|^2 \alpha_{2,j} + \sigma_n^2}. \quad (15)$$

The rate of strong and weak user in SBD-NOMA across any sub-band is given by

$$R_{im} = W_{sb} \sum_{j=1}^{P/2} \log_2 (1 + SINR_{i,j}); i \in \{1, 2\}, \quad (16)$$

wherein W_{sb} is the sub-band bandwidth.

The summation of P users over all sub-bands m is K , where $K \in \xi$ is the total number of users and it belongs to the set ξ . In other words, we can say that $n \in J \wedge J \in \xi$. The total sum rate of the system is given by

$$R_{sum} = \sum_{i=1}^2 \sum_{m=1}^{K/P} R_{im}. \quad (17)$$

Finally, the sum capacities of conventional OMA is written as,

$$R_{i,OMA} = W/K \sum_{k=1}^K \log_2 \left(1 + \frac{|\mathbf{z}_{i,k} \cdot \mathbf{h}_{i,k}|^2 \alpha_{i,k}}{\sigma_k^2} \right), \quad (18)$$

From (17), it can be seen that the user power has a direct effect not only on individual user data rate but also on the SINR of other users, which shows the importance of power allocation in SBD-NOMA system.

2.4. Channel Allocation Algorithm

In the proposed UL SBD-NOMA scheme, both conventional OMA and NOMA techniques are implemented simultaneously, therefore, the question of users selection in a set is important. This is because the user pairing has the potential of reducing the complexity at the receiver side. The user pairing strategy affects the overall throughput of the proposed scheme. Careful user pairing not only improves the sum rate, but also has the potential to improve the individual user rates. The grouping is done on the basis of the channel gains between the users. The pairwise orthogonal users are grouped together in the same sub-band to get full benefit of the NOMA within each sub-band. The proposed user pairing algorithm reduces the number of MUD required at the receiver side. It also offers reduced interference by removing inter cluster and inter set interference. It also eliminates the need of complex receiver designing, which reduces the cost and also provide enhanced quality-of-service (QoS). The detailed algorithm for choosing the members of strong and weak set is presented in Table 1. The algorithm aims to minimize the interference offered by the weak users to the strong users.

Table 1. Sets Formation and Subchannel Allocation Algorithm

Initialization
1 A set ξ of K users, where $K = \{1, \dots, k\}$. 2 Subchannel Allocation Matrix, $\mathbf{M} = \mathbf{0}_{(K \times N)}$. 3 Number of antennas, N .
Channel Allocation
Step 1) BS creates \mathbf{M} from reported CSI values, $\mathbf{M} = \{\mathbf{h}_1, \mathbf{h}_2, \dots, \mathbf{h}_K\}$. Step 2) The channel gains are sorted in descending order, forming a set \mathbf{M}_{ord} . $\mathbf{M}_{ord} = \{ \mathbf{h}_1 ^2, \mathbf{h}_2 ^2, \dots, \mathbf{h}_K ^2\}$ where $ \mathbf{h}_K ^2 > \mathbf{h}_{K+1} ^2$ and $K \in \{1, 2, \dots, k\}$. Step 3) The parent set is split into two halves $\mathbf{H}_1 = \{ \mathbf{h}_1 , \mathbf{h}_2 , \dots, \mathbf{h}_{\lfloor K/2 \rfloor} \}$, $\mathbf{H}_2 = \{ \mathbf{h}_{\lfloor K/2 \rfloor + 1} , \mathbf{h}_{\lfloor K/2 \rfloor + 2} , \dots, \mathbf{h}_K \}$, $\lfloor \cdot \rfloor$ denotes the floor function. The first half is taken to be a strong set A while the other is a weak set B . In \mathbf{H}_1 , the N users having the higher channel gains are paired. Similarly, in \mathbf{H}_2 , the N users having lower channel gains are paired. $\mathbf{H}_1 = \{ \mathbf{h}_{1,1} , \mathbf{h}_{1,2} , \dots, \mathbf{h}_{1,\lfloor K/2 \rfloor} \}$, $\mathbf{H}_2 = \{ \mathbf{h}_{2,\lfloor K/2 \rfloor + 1} , \mathbf{h}_{2,\lfloor K/2 \rfloor + 2} , \dots, \mathbf{h}_{2,K} \}$, Step 4) Pair orthogonal users head to tail. Step 5) For SBD-NOMA, each Rayleigh fading channel matrix divides itself into smaller matrices with dimension $(N \times P/2)$, where P denotes the access scheme. The smaller channel matrices and the corresponding user indexes of strong and weak sets satisfy the condition $\sum_{m=1}^{K/P} A_m \cup B_m = \xi$. Go to 5).
End When all the N users from the two sets are paired in sub-bands.
Note: The subscript i representing the index of being strong and weak set has been introduced in the definition of channel gains for notational consistency and clarification.

3. POWER ALLOCATION

In the previous section, constant power allocation coefficients are considered. By constant power allocation coefficients, we mean that both users (i.e., strong and weak users) have equal power. In this case, we have not followed the conventional power allocation policy which states that allocates more transmit power to the users with poor channel conditions (i.e., weak users) and less transmit power to the users with better channel conditions (i.e., strong users) to set power difference between the users that allows post coding to suppress or minimize the interference and exploits the gain from NOMA within users. However, in this section, more sophisticated choices of power allocation are considered. In this section, we worked on

giving unequal power allocation coefficients to NOMA on the basis of instantaneous channel conditions. This helps in further improving the performance of MIMO-NOMA system. However, dividing the users into orthogonal groups cannot exploit the full potential of NOMA with the exception that the complexity at the receiver side is reduced. This leads to the formation of SBD-NOMA system with optimal power allocation. The main purpose is to maximize the sum rate across all sub-bands by allocating optimal power and also provide some degree of fairness to each user. The corresponding resource allocation problem considers the number of users in each sub-band, the choice of user pairing and the power allocated to each sub-band. The framed optimization problem maximizes the sum rate while also ensures fairness in the system. For the sake of simplicity, we are assuming two users in each sub-band while the total number of users is K . Instead of allocating power values to each sub-band through iterative water filling, the power allocated across each sub-band is assumed to be equally allocated, which would reduced the signaling overhead and complexity of the proposed numerical solutions. However, in general, the sum rate is not convex in nature for more than two transmitting sources, hence, the solution is proposed here for NOMA₂.

*

Lemma 1: The achievable sum rate of the system is concave in nature for more than two transmitting sources.

Proof: See Appendix A.

Mathematically, the problem is formulated as

$$\begin{aligned} & \underset{\alpha_{i,j}}{\text{maximize}} && R_{im} \\ & \text{subject to} && \alpha_{1,j} + \alpha_{2,j} \leq P_T, \forall j \\ & && \alpha_{i,j} \geq 0, \forall i, \forall j \\ & && R_{im,j} \geq r_{min}, \text{ where } j \in J, \end{aligned} \quad (19)$$

where (19) represents the constraints of the framed optimization problem, P_T is the total power allocated to users within a particular sub-band, R_{im} represents the data rate across each sub-band, $R_{im,j}$ represents the individual data rate of j^{th} user and r_{min} represents the minimum target rate to maintain fairness among the users. The users are already paired and are chosen from two distinct sets

to reduce the inter-set interference. Taking into account the objective function described above and solving the optimization problem through Lagrange multipliers leads to the following formulation of the objective function denoted by F , i.e.,

$$\begin{aligned} F = & R_{im} + \sum_{j=1}^{P/2} \lambda_j (P_T - \alpha_{1,j} - \alpha_{2,j}) + \\ & \sum_{j=1}^{P/2} \kappa_j (R_{1m,j} - r_{min}) + \sum_{j=1}^{P/2} \tau_j (R_{2m,j} - r_{min}), \end{aligned} \quad (20)$$

where λ_j , κ_j and τ_j represent the Lagrange multipliers. Using the standard procedure, by differentiating F with respect to all $\alpha_{1,j}$ and $\alpha_{2,j}$ and by setting them equal to zero, we obtain a set of $5|J|$ non-linear equations having $5|J|$ unknowns, where $|J|$ denotes the cardinality of set J . For the sake of simplicity, the derivatives here are taken only for $\alpha_{1,j}$, $\alpha_{2,j}$, τ_j , λ_j and κ_j . A similar procedure can be used for other variables as well. The entire procedure is repeated over all sub-bands to maximize the overall sum rate. We obtain

$$\begin{aligned} \partial F / \partial \alpha_{1,j} = & \frac{W_{sb} \|\mathbf{z}_{1,j} \cdot \mathbf{h}_{1,j}\|^2}{\|\mathbf{z}_{1,j} \cdot \mathbf{h}_{2,j}\|^2 \alpha_{2,j} + \sigma_j^2 + \|\mathbf{z}_{1,j} \cdot \mathbf{h}_{1,j}\|^2 \alpha_{1,j}} \\ & - \lambda_j - \kappa_j \frac{W_{sb} \|\mathbf{z}_{1,j} \cdot \mathbf{h}_{1,j}\|^2}{\|\mathbf{z}_{1,j} \cdot \mathbf{h}_{2,j}\|^2 \alpha_{2,j} + \sigma_j^2 + \|\mathbf{z}_{1,j} \cdot \mathbf{h}_{1,j}\|^2 \alpha_{1,j}}, \end{aligned} \quad (21)$$

$$\begin{aligned} \partial F / \partial \alpha_{2,j} = & \frac{\|\mathbf{z}_{2,j} \cdot \mathbf{h}_{2,j}\|^2}{\|\mathbf{z}_{2,j} \cdot \mathbf{h}_{2,j}\|^2 \alpha_{2,j} + \sigma_j^2} - \lambda_j \\ & - \frac{W_{sb} \|\mathbf{z}_{1,j} \cdot \mathbf{h}_{1,j}\|^2 \|\mathbf{z}_{1,j} \cdot \mathbf{h}_{2,j}\|^2 \alpha_{1,j}}{\|\mathbf{z}_{1,j} \cdot \mathbf{h}_{2,j}\|^2 \alpha_{2,j} + \sigma_j^2 + \|\mathbf{z}_{1,j} \cdot \mathbf{h}_{1,j}\|^2 \alpha_{1,j} \varphi} \\ & + \kappa_j \frac{W_{sb} \|\mathbf{z}_{1,j} \cdot \mathbf{h}_{1,j}\|^2 \|\mathbf{z}_{1,j} \cdot \mathbf{h}_{2,j}\|^2 \alpha_{1,j}}{\|\mathbf{z}_{1,j} \cdot \mathbf{h}_{2,j}\|^2 \alpha_{2,j} + \sigma_j^2 + \|\mathbf{z}_{1,j} \cdot \mathbf{h}_{1,j}\|^2 \alpha_{1,j} \varphi} \\ & + \tau_j \frac{W_{sb} \|\mathbf{z}_{2,j} \cdot \mathbf{h}_{2,j}\|^2}{\sigma_j^2}, \end{aligned} \quad (22)$$

where $\varphi = \|\mathbf{z}_{1,j} \cdot \mathbf{h}_{2,j}\|^2 \alpha_{2,j} + \sigma_j^2$.

$$\partial F / \partial \lambda_j = P_T - \alpha_{1,j} - \alpha_{2,j}, \quad (23)$$

* The numerical solution for other schemes is not proposed here due to duality gap in transformation from non-convex to convex function.

$$\partial F / \partial \kappa_j = W_{sb} \log_2 \left(1 + \frac{\|\mathbf{z}_{1,j} \cdot \mathbf{h}_{1,j}\|^2 \alpha_{1,j}}{\|\mathbf{z}_{1,j} \cdot \mathbf{h}_{2,j}\|^2 \alpha_{2,j} + \sigma_j^2} \right) - r_{min}, \quad (24)$$

$$\partial F / \partial \tau_j = W_{sb} \log_2 \left(1 + \frac{\|\mathbf{z}_{2,j} \cdot \mathbf{h}_{2,j}\|^2 \alpha_{2,j}}{\sigma_j^2} \right) - r_{min}, \quad (25)$$

$$\alpha_{1,j} \cdot \partial F / \partial \alpha_{1,j} = 0, \quad (26)$$

$$\alpha_{2,j} \cdot \partial F / \partial \alpha_{2,j} = 0, \quad (27)$$

$$\lambda_j \cdot \partial F / \partial \lambda_j = 0, \quad (28)$$

$$\kappa_j \cdot \partial F / \partial \kappa_j = 0, \quad (29)$$

$$\tau_j \cdot \partial F / \partial \tau_j = 0, \quad (30)$$

where $\alpha_{1,j}, \alpha_{2,j}, \lambda_j, \kappa_j, \tau_j \geq 0$. Solving the above Equation (21) for the Lagrange variable λ_j , and substituting it in (22) and the value of $\alpha_{2,j}$ from (23) gives the value of $\alpha_{1,j}$. The $\alpha_{1,j}$ turns out to be

$$\alpha_{1,j} = \frac{2(\varphi_{aj} - \varphi_{cj})\varphi_{bj}(\varphi_{bj}(1 + \tau_j)(\sigma_j^2 + \varphi_{cj}P_T) + \varphi_{aj}(1 + \kappa_j)(\Psi_1))}{2(\varphi_{bj})^2(\varphi_{aj} - \varphi_{cj})(\varphi_{cj} + \varphi_{aj}\kappa_j - \varphi_{aj}\tau_j + \varphi_{cj}\tau_j)} - \frac{2\sqrt{\varphi_{aj}(\varphi_{aj} - \varphi_{cj})\varphi_{bj}^2(1 + \kappa_j)(1 + \tau_j)(\sigma_j^2(-\varphi_{cj} + \varphi_{bj}) + \varphi_{aj}(\Psi_1))^2}}{2(\varphi_{bj})^2(\varphi_{aj} - \varphi_{cj})(\varphi_{cj} + \varphi_{aj}\kappa_j - \varphi_{aj}\tau_j + \varphi_{cj}\tau_j)}, \quad (31)$$

where $\Psi_1 = (\sigma_j^2 + \varphi_{bj}P_T)$, φ_{aj} , φ_{bj} and φ_{cj} are given by $\varphi_{aj} = \|\mathbf{z}_{1,j} \cdot \mathbf{h}_{1,j}\|^2$, $\varphi_{bj} = \|\mathbf{z}_{2,j} \cdot \mathbf{h}_{2,j}\|^2$ and $\varphi_{cj} = \|\mathbf{z}_{1,j} \cdot \mathbf{h}_{2,j}\|^2$. The value of $\alpha_{2,j}$ is derived by substituting the value of $\alpha_{1,j}$ in (23) and is given by

$$\alpha_{2,j} = P_T - \alpha_{1,j}. \quad (32)$$

†

† In order to present the general idea, we derive the expression of $\alpha_{1,j}$ in terms of Lagrange variables. However, the values of $\alpha_{1,j}$ are numerically solved in MATLAB and the expressions of Lagrange variables are explicitly not added in the paper.

3.1. Extension to SBD-NOMA with P users in each sub-band

To investigate the scenario of more than two users in each sub-band, multistage power allocation is proposed. In the first stage, the users form two distinct sets A and B on the basis of algorithm presented in Table I. After this step, two sub-bands from sets A and B are formed, each having equal number of users. The power allocated to each sub-band is equal to half of the total transmission power. In this scenario, the channel gains become the sum of all channel powers in the two sub-bands. The same procedure for SBD-NOMA₂ is repeated for power allocation within the two sub-bands. In the second stage, the two sub-bands further divide themselves into smaller sub-bands, i.e., two sub-bands are formed in each sub-band of the previous stage with the total power per sub-band as determined in the first stage. In the third stage, these sub-bands further divide into smaller sub-bands to allocate power to all users. The procedure is repeated until all users are allocated with an optimal transmission power.

The procedure presented above is also applicable to the numbers of users, which are not in power of 2. To illustrate the concept, consider $K = 12$, i.e., the total number of users is 12, which is not a power of 2. However, the users can easily be split into three sub-bands having four users each. In the second stage, these four users further divide themselves into two sub-bands having two users in each sub-band. After that the power allocation proposed in section 3 can easily be applicable to the users. For other even number of users, there are many possible combinations. For e.g., consider $K = 26$, the users can be split into two sub-bands having thirteen users each or seven sub-bands can be form having four users in six sub-bands and the remaining two users can be incorporated in the last one, thirteen sub-bands of two users can also be form. However, in the examples presented above, the number of strong and weak users in the sub-bands may not be equal and even. There are many possible combinations of grouping in the examples presented above, which is beyond the scope of this paper. The general expression for power allocation in this scenario is given below

$$\sum_{j=1}^{P/2} \alpha_{i,j} = P_T, \forall i. \quad (33)$$

It must be noticed that the constraints in (19) and (33) is the same. The (33) gives the same result on expanding the summation for two users over J , which varies from 1 to $P/2$. However, (19), is written for just two users, while the constraint has been generalize in (33).

4. OUTAGE PROBABILITY

The outage probability is an important performance metric as it measures the probability of unsuccessful signal decoding for a given service. The outage probability experienced by any n^{th} user in weak set can be defined as

$$\begin{aligned} P_o &= 1 - Pr(SINR_{2,n} > r_{min}) \\ &= 1 - Pr\left(\frac{|\mathbf{h}_{2,n} \cdot \mathbf{z}_{2,n}|^2 \alpha_{2,n}}{\sigma_n^2} > r_{min}\right), \end{aligned} \quad (34)$$

Building on the above Equation (34), the outage probability experienced by any n^{th} user in strong set can be written as,

$$\begin{aligned} P_o &= 1 - Pr(SINR_{1,n} > r_{min}) \\ &= 1 - Pr\left(\frac{|\mathbf{h}_{1,n} \cdot \mathbf{z}_{1,n}|^2 \alpha_{1,n}}{\sum_{j=1}^{P/2} |\mathbf{h}_{2,j} \cdot \mathbf{z}_{1,n}|^2 \alpha_{2,j} + \sigma_n^2} > r_{min}\right), \end{aligned} \quad (35)$$

In the above expressions, there is no intra-set interference. Here, it is assumed that the BS is equipped with N antennas and, hence, the number of interferers from the weak set are also N , therefore, it may be stated that the strong users are only affected by inter-set interference from the weak users. Furthermore, $\mathbf{Z}_2 \mathbf{H}_2 = \mathbf{I}_k$ and $\mathbf{z}_{2,n} \mathbf{h}_{2,j} = \delta_{nj}$ where $\delta_{nj} = 1$ for $n = j$ and 0 otherwise. The same holds true for the strong users as well. We first derive the approximate PDF of the SINR of the users in strong and weak sets, respectively.

4.1. Approximate PDF of SINR for weak users

To derive the PDF of the SINR of weak users, the SINR given by (14), can be written as,

$$SINR_{2,n} = \frac{\alpha_{2,n}}{\sigma_n^2} \triangleq \frac{\alpha_{2,n}}{\|\mathbf{z}_{2,n}\|^2 \sigma^2} \triangleq \frac{\alpha_{2,n}}{[(\mathbf{H}_2^* \mathbf{H}_2)^{-1}]_{nn} \sigma^2}. \quad (36)$$

Denoting the SINR defined in (36) with a random variable (RV) Y , it becomes

$$SINR_{2,n} = \frac{\alpha_{2,n}}{Y \sigma^2}, \quad (37)$$

where $Y = [(\mathbf{H}_2^* \mathbf{H}_2)^{-1}]_{nn}$. From (37), it is obvious that we can derive the PDF of SINR provided that the PDF of Y is known. The RV Y in the denominator of (37) is expanded as

$$[(\mathbf{H}_2^* \mathbf{H}_2)^{-1}]_{nn} = \frac{1}{(\mathbf{h}_{2,n})^* \mathbf{h}_{2,n} - (\mathbf{h}_{2,n})^* \mathbf{H}_{2n} (\mathbf{H}_{2n}^* \mathbf{H}_{2n})^{-1} \mathbf{h}_{2,n} (\mathbf{H}_{2n})^*}, \quad (38)$$

where \mathbf{H}_{2n} is the sub matrix obtained after removing the n^{th} column from the matrix \mathbf{H}_2 . Hence,

$$SINR_{2,n} = \frac{\alpha_{2,n} (\mathbf{h}_{2,n})^* \mathbf{h}_{2,n} - (\mathbf{h}_{2,n})^* \mathbf{H}_{2n} (\mathbf{H}_{2n}^* \mathbf{H}_{2n})^{-1} \mathbf{h}_{2,n} (\mathbf{H}_{2n})^*}{\sigma^2}. \quad (39)$$

Generally, for any $N \times K$ Rayleigh fading matrix, the expression in the numerator of (39) follows a gamma distribution with shape parameter $N - K + 1$ and scale parameter 1, i.e., $\Gamma(N - K + 1, 1)$. This is because it represents sum of independent and identically distributed (i.i.d.) exponential RVs each having a unit mean and the PDF is given as

$$f_Y(y) = \frac{y^{(N-K)} \exp(-y)}{\Gamma(N - K + 1)}. \quad (40)$$

However, in the above case, there are N users in each set and the channel gains are Rayleigh faded with path loss. Therefore, the expression in the numerator of (39) follows a gamma distribution with shape parameter 1 and scale parameter λ_{in} i.e., $\Gamma(1, \lambda_{in})$, where λ_{in} is the mean power experienced by the n^{th} user because of path loss. The $\Gamma(1, \lambda_{in})$, with shape parameter 1 converges to an exponential distribution given by

$$f_Y(y) = \frac{1}{\lambda_{in}} \exp\left(\frac{-y}{\lambda_{in}}\right), \quad (41)$$

Multiplication with power allocation coefficient $\alpha_{2,n}$ and division by the noise variance σ^2 , both of which are constants for a particular user will only change the mean parameter of the RV Y . Hence, the final closed-form expression for the PDF of the SINR of weak user becomes

$$f_Y(y) = \frac{1}{\tau_{in}} \exp\left(\frac{-y}{\tau_{in}}\right), \quad (42)$$

where τ_{in} is the modified mean. To calculate the outage, first find the coverage probability by integrating the above expression. we have

$$Pr(SINR_{2,n} > r_{min}) = \int_{r_{min}}^{\infty} f_Y(y) dy. \quad (43)$$

Using (34), we obtain the outage probability of weak users.

$$\begin{aligned} P_o &= 1 - Pr(SINR_{2,n} > r_{min}), \\ &= 1 - \int_{r_{min}}^{\infty} f_Y(y) dy. \end{aligned} \quad (44)$$

4.2. Approximate PDF of SINR for strong users

To derive the PDF of SINR of strong users, the SINR given by (8) can be written as

$$\begin{aligned} SINR_{1,n} &= \frac{\alpha_{1,n}}{\sum_{j=1}^{P/2} |\mathbf{h}_{2,j} \cdot \mathbf{z}_{1,n}|^2 \alpha_{2,j} + |\mathbf{z}_{1,n}|^2 \sigma^2} \\ &\triangleq \frac{\alpha_{2,n}}{\sum_{j=1}^{P/2} |\mathbf{h}_{2,j} \cdot \mathbf{z}_{1,n}|^2 \alpha_{2,j} + [(\mathbf{H}_1^* \mathbf{H}_1)^{-1}]_{nn} \sigma^2}. \end{aligned} \quad (45)$$

Denoting the SINR defined in (45) with RV X and T , it becomes

$$SINR_{1,n} = \frac{\alpha_{1,n}}{X + T\sigma^2}, \quad (46)$$

where $T = [(\mathbf{H}_1^* \mathbf{H}_1)^{-1}]_{nn}$. To calculate the PDF of the SINR of strong users, we need to calculate the PDF of the RV X and T . The PDF of the product of $T\sigma^2$ is already known from above. To derive the density function of interference represented by X , notice that X is a sum of exponential RVs and its PDF is given by Gamma distribution, i.e.,

$$X = \sum_{j=1}^{P/2} \|\mathbf{z}_{1,n} \cdot \mathbf{h}_{2,j}\|^2 \alpha_{2,j}, \quad (47)$$

$$f_X(x) = \frac{x^{(v-1)} \exp(-x/\Omega)}{\Gamma(v) \Omega^v}, \quad (48)$$

where $v = \frac{\mathbb{E}[X]^2}{\text{var}[X]}$ and $\Omega = \frac{\text{var}[X]}{\mathbb{E}[X]}$. To derive the analytical expressions for v and Ω , we assume independent interfering signals from weak users, where the power allocation coefficient $\alpha_{2,j}$ is considered as a constant for a particular user. Hence, the mean and variance of X can

be written as

$$\mathbb{E}[X] = \sum_{j=1}^{P/2} \alpha_{2,j} \mathbb{E}[W_j], \quad (49)$$

where $W_j = \varphi_{c j n} = \|\mathbf{z}_{1,n} \cdot \mathbf{h}_{2,j}\|^2$ and

$$\text{var}(X) = \sum_{j=1}^{P/2} \alpha_{2,j}^2 \text{var}(W_j). \quad (50)$$

It can be seen that the PDF of W_j is also gamma distributed with unit scale parameter. The general expression of the PDF for the case $N \geq K$ can be written as,

$$f_W(w) = \frac{K^{N-K+1} \exp(-Kx) w^{N-K}}{\Gamma(N-K)}, \quad (51)$$

$$\mathbb{E}(W_j) = 1, \quad (52)$$

$$\text{var}(W_j) = 1. \quad (53)$$

Therefore, the values of v and Ω are given by

$$v = \frac{(\sum_{j=1}^{P/2} \alpha_{2,j})^2}{\sum_{j=1}^{P/2} \alpha_{2,j}^2}, \quad (54)$$

and

$$\Omega = \frac{\sum_{j=1}^{P/2} \alpha_{2,j}^2}{\sum_{j=1}^{P/2} \alpha_{2,j}}. \quad (55)$$

Using (54) and (55), PDF of X can be computed. The PDF of the product $T\sigma^2$ is already known. The addition of two independent gamma random variables is also gamma distributed. The numerator of (45) is just a power allocation coefficient $\alpha_{1,n}$, which is considered as a constant, hence, just change the scale parameter of resultant gamma distribution. Therefore, the final expression for the PDF of SINR can be written as

$$f_U(u) = \frac{u^{(s-1)} \exp(-u/\Omega_w)}{\Gamma(s) \Omega_w^s}, \quad (56)$$

where s and Ω_w are the resultant shape and scale parameters, respectively. To calculate the outage, we have

$$Pr(SINR_{1,n} > r_{min}) = \int_{r_{min}}^{\infty} \frac{u^{(s-1)} \exp(-u/\Omega_w)}{\Gamma(s) \Omega_w^s} du, \quad (57)$$

Equation (57) can be expanded as

$$\exp\left(\frac{-r_{min}}{\Omega_w}\right) \sum_{f=0}^s \frac{\left(\frac{r_{min}}{\Omega_w}\right)^f}{f!}. \quad (58)$$

By using the above equation, we can calculate the coverage probability. Hence, by using (35), the outage probability of strong users can be obtained.

$$\begin{aligned} P_o &= 1 - Pr(SINR_{1,n} > r_{min}), \\ &= 1 - \exp\left(\frac{-r_{min}}{\Omega_w}\right) \sum_{f=0}^s \frac{\left(\frac{r_{min}}{\Omega_w}\right)^f}{f!}. \end{aligned} \quad (59)$$

The outage equations given by (43) and (57) depends upon the number of transmit and receive antennas, the threshold chosen for estimating outage probability, the number of users in each strong and weak set and the interference term appearing in the denominator of SINR. Here, it can be seen that the interference term will greatly effect the overall outage probability of the users.

5. PERFORMANCE EVALUATION

In this section, simulation results of the scenarios under discussion are presented. We investigate the performance of the SBD-NOMA and compare it with the conventional OMA and NOMA techniques, with a fixed set of power allocation coefficient. The cell radius is assumed to be 1000m in which all the users are randomly distributed. The value of the radius is chosen only for a fair comparison between different SBD schemes under discussion. The channel coefficients are assumed to be i.i.d Rayleigh flat faded. The transmission power per users is 24dBm. The noise is assumed to be zero mean circular-symmetric complex Gaussian having a noise density of -174dBm/Hz . The overall system bandwidth is 4.32MHz. The path loss is calculated by using the following model

$$PL_{dB} = 30 + 10\beta \log_{10}(d), \quad (60)$$

where d is the distance between the BS and the MS and β is the path loss exponent, which is kept at 4 in this study.

Fig. 2 demonstrates the relationship between sum capacity and varying the number of users, K . The figure compares the sum capacity of OMA, NOMA and

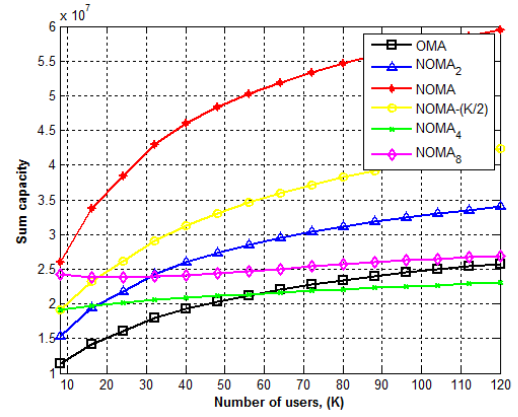


Figure 2. Sum capacity comparison between SBD-NOMA, conventional OMA and NOMA techniques.

proposed SBD-NOMA schemes each having a fixed set of power allocation coefficients. The primary observation is examining the effect of number of users on sum capacity in SBD-NOMA. The sum capacity improves with the increase in the number of users but the improvement is not substantial for NOMA₄ and NOMA₈ schemes after the number of users exceed a certain limit, because of significant interference. However, these schemes offer better coverage probability and hence their outage probability is quite low and they offer less complexity than the conventional NOMA technique. The inconsistency in performance is because of the reason that SBD-NOMA can reduce the achievable rates as dividing the entire bandwidth into sub-bands cannot exploit the full potential of NOMA, where all users can occupy the entire bandwidth. As bandwidth is directly proportional to each user's data rate, the effect is visible in the sum capacity analysis. However, dividing the users into orthogonal groups will reduce the intra-set interference. The major outcome of sharing is that the sum rate is expected to improve, which can be further enhanced by properly allocating power to weak users. Also it can be noticed that OMA techniques have a very poor spectrum fairness index among the users. This is because there is exclusivity in resource allocation, i.e., a resource block allocated to one user can not be used by any other user. However, the fairness offered by SBD-NOMA is way better than OFDMA with reduced complexity and signaling overhead at the BS. To compare the fairness in SBD-NOMA, NOMA and OMA techniques, modified

Jain's fairness index (MJFI) can be evaluated, which is given as

$$MJFI = \frac{(\sum_{k=1}^{K/2} \bar{R}_{i,k})^2}{K/2 \sum_{k=1}^{K/2} \bar{R}_{i,k}^2}, i \in \{1, 2\}, \bar{R}_{i,k} = \frac{R_{i,k}}{R_{i,k}^{max}}, \quad (61)$$

where $R_{i,k}^{max}$ is the maximum rate of the k^{th} user when there are no other users in the system i.e., it is calculated by doing single user iterative water filling. As a result, the rate offered by conventional OMA is minimum but its outage probability is low, which increases the overall outage capacity of the conventional OMA system. The *outage capacity* is defined as the maximum rate that can be maintained by each user multiplied with the success probability of the users. It shows a clear picture of system performance for both data rates and success of each user. The outage capacity analysis of SBD-NOMA is evaluated in Fig. 3. SBD-NOMA performs well in terms of outage capacity as shown. We can derive an interesting result by combining Fig. 2 and 3 that although the conventional UL NOMA achieves maximum sum capacity but it increases the receiver complexity and outage probability to a great extent, which is practically not desired especially if the number of users in a system is large. The same reason lies behind the intersection of curves in Fig.3. As it can be seen from Fig.2 that NOMA offers higher data rates and its sum capacity generally improves with the increase in the number of users. However, by incorporating more users within the same sub-band, the intra-set interference increases. Therefore, NOMA has high outage probability. Although, the other schemes offer better coverage probability and hence their outage probability is quite low and they offer less complexity than the conventional NOMA technique but their data rates are low. By combining the two parameters, the curves intersect in Fig.3. Hence, in the situations, where the priority is reduced receiver complexity, cost and enhanced QoS, SBD-NOMA schemes should be preferred over conventional UL NOMA that provide better rate and a fairly reliable transmission scheme.

Fig. 4 reveals the energy efficiency (EE) of a hybrid SBD-NOMA scheme with increasing number of users. *Energy Efficiency* (η_{EE}) defined in bits/sec/Watt, is the amount of energy required by the system to transmit data and is expressed as

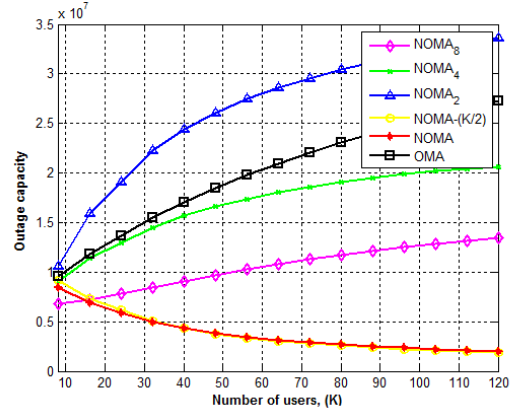


Figure 3. Outage capacity of OMA, NOMA and proposed SBD scheme.

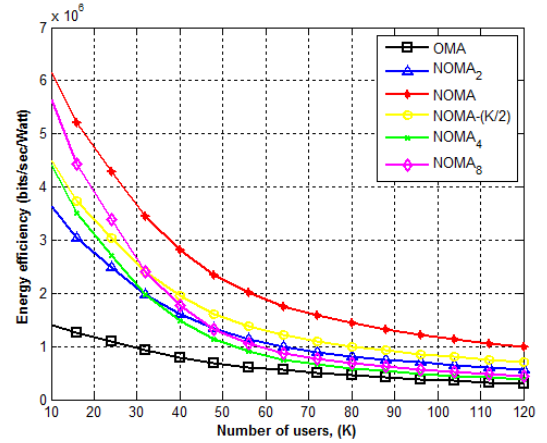


Figure 4. Energy efficiency of SBD-NOMA with OMA and NOMA technique.

$$\eta_{EE} = \frac{R_{sum}}{P_T} = \frac{\sum_{m=1}^{K/P} \sum_{j=1}^{P/2} W_{sb} \log_2 (1 + SINR_{i,j})}{P_T}, \quad (62)$$

where P_T is the total transmit power of the system. The trend shows that as the number of users increases, the total transmit power increases, thus there is an increase in the total sum rate. However, there is a reduction in the EE with increasing number of users.

In Fig. 5, the impact of cell radius on the performance of OMA, NOMA and SBD-NOMA is demonstrated. It can be seen that SBD-NOMA performs better than the conventional NOMA if the cell radius is assumed to be very small. However, NOMA outperforms at other values, but as the cell radius increases, the inter-set interference

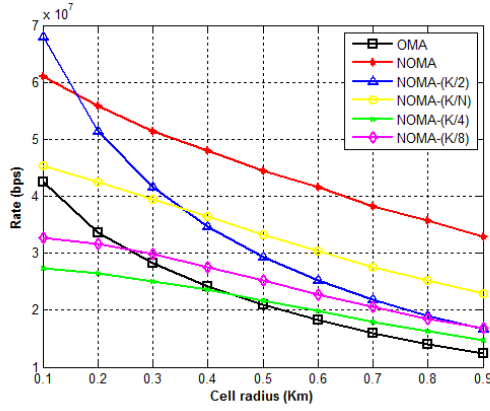


Figure 5. Impact of cell radius on SBD scheme (N=2, K=40).

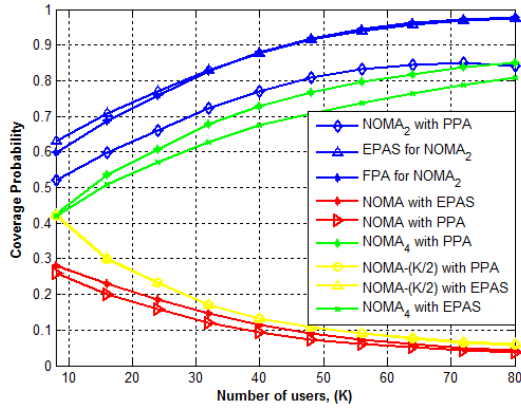


Figure 6. Coverage probability comparison of NOMA₂ with different power allocation schemes and NOMA technique.

offered to NOMA by weak set also enhances, which increases the decoding complexity at the receiver side.

Fig. 6 depicts the coverage probability of conventional NOMA and SBD-NOMA with different power allocation schemes. *Coverage probability* is defined as the probability that a certain number of users achieves a data rate greater than the target data rate. It can be easily seen that SBD-NOMA performs well as compared to NOMA in terms of coverage probability. The coverage probability of FPA and EPAS is even better in this case as compared to the proposed approach, however, EPAS being the simplest criteria of allocating power to users does not perform well, as it allocates equal power to all users and therefore treats the weak users in the same manner as the strong ones. The SBD-NOMA provides every pair a power that suits their channel gain, which allows a balance between the required power, fairness and the target rate with total power

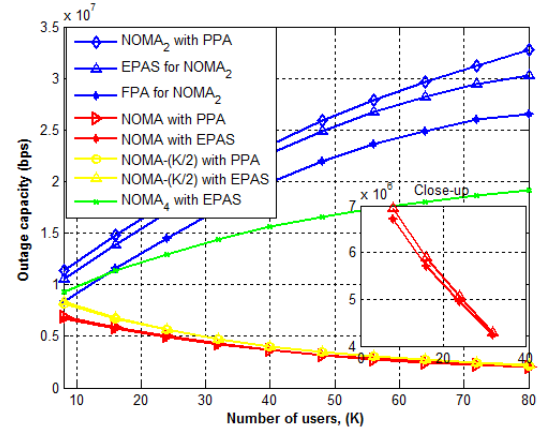


Figure 7. Outage capacity comparison of NOMA₂ with different power allocation schemes and NOMA technique.

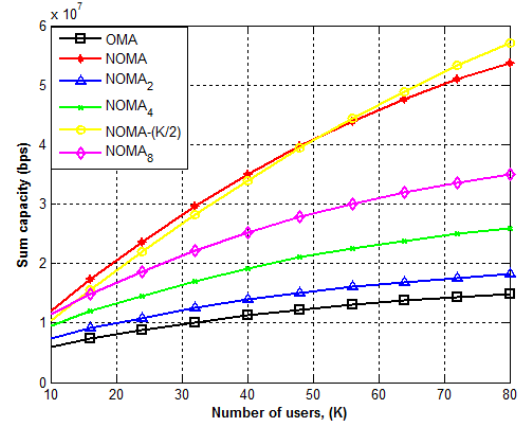


Figure 8. Sum capacity comparison of SBD-NOMA for $K \geq N$.

allocation constraint across each sub-band. Although, the optimal NOMA scheme shows greater sum rate but its coverage probability in this scenario is less than the optimal solution. The same trend is depicted in the Fig.6.

Fig. 7 shows the outage capacity of SBD-NOMA with conventional NOMA scheme. The outage capacity is larger for SBD-NOMA₂ with the proposed power allocation scheme. However, with equal power allocation, the system treats the weak users in the same way as strong users. As strong users get significant interference from weak users, hence, the capacity of strong users gets degraded. The optimal power allocation in SBD-NOMA ensures fairness in the system by imposing an upper limit on each user's individual data rate as compared to EPAS and FPA schemes. From this figure, it is clear that the proposed power allocation scheme performs better than the existing ones.

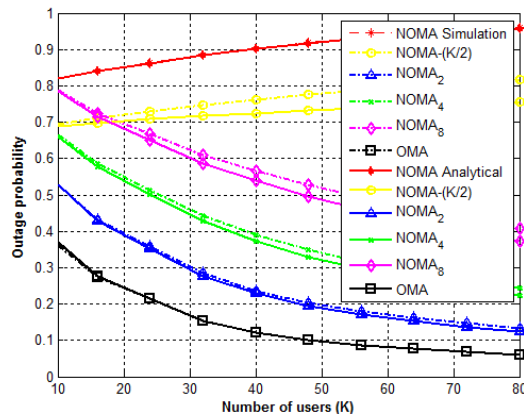


Figure 9. Outage probability of SBD-NOMA for $K \geq N$.

Fig. 8 and 9 depict the sum capacity and outage probability of SBD-NOMA with no intra-set interference. It can be observed from the figure that with no intra-set interference, the sum rate is inversely proportional to the number of sub-bands. However, $\text{NOMA}_{K/2}$ nominates NOMA with increasing number of users. This is because of minimum weak set interference. The outage probability for $K \geq N$ is less as compared to the conventional SBD-NOMA discussed above. The same trend is shown in the figure.

6. CONCLUSION

This paper investigated the performance of SBD-NOMA, which is an OFDMA-based NOMA system with other multiple access schemes, OMA and NOMA. It can be seen that in general, NOMA has more decoding complexity. It introduces some controllable interferences at the receiver to realize overloading due to which it can support massive connectivity and higher spectral efficiency. It also requires greater number of SIC for decoding, which requires complex receiver designing. The complexity of SBD-NOMA lies between NOMA and OMA. The depth of SIC in SBD-NOMA is much less than the NOMA system. It also requires receiver of moderate complexity. SBD-NOMA sum rate also lies midway between NOMA and OMA. However, it offers minimum error variance because of reduced depth of SIC and moderate receiver complexity. OMA, on the other hand offers least complexity and is therefore a reasonable choice for achieving good system level throughput in packet domain services using channel

aware time and frequency domain scheduling. However, OMA cannot provide the further enhancements in quality of experience required at the cell edge user. Also, MIMO NOMA offers larger sum rate capacity as compared to MIMO OMA except when there is a single user. The reason behind the larger sum rate is the power split for which MIMO NOMA achieves larger sum rates. Hence, in a situation where user requirement is reduced complexity, enhanced rates, better quality of service and a fairly reliable transmission schemes, SBD-NOMA should be preferred. In situations, where user requirement is higher sum rates, NOMA should be preferred as BS can easily cope with decoding complexity as it has more power. In situations, where user requirement is reduced rates with no interference and simple single user detection, OMA is preferred. The paper also discussed the approximate closed-form expressions for the outage probability of strong and weak users in SBD-NOMA. The results presented herein paint a favorable picture that SBD-NOMA performs better than NOMA in terms of achievable rates. The proposed SBD scheme also offered better sum rates with reduced complexity especially in massive access scenarios. The proposed scheme with under different path loss and power allocation outperformed the EPAS and FPA schemes.

7. ACKNOWLEDGEMENT

This work was funded, in part, by the Ministry of Education and Science of the Russian Federation Grant No. 02.G25.31.0190 dated 04.27.2016 and performed in accordance with Russian Government Resolutions No. 218 of 09.04.2010. Authors also acknowledged the contribution of the COST Action on Inclusive Radio Communications (IRACON) CA15104.

A. PROOF OF LEMMA 1

The achievable sum rate of the system given by (17) is expanded as

$$R_{sum} = \frac{1}{\ln 2} \sum_m W_{sb} R_{rr}, \quad (63)$$

where

$$R_{rr} = \ln \left(\sum_{j=1, j \neq n}^{P/2} \varphi_{bjn} \alpha_{2,j} + \sigma_n^2 + \varphi_{bn} \alpha_{2,n} \right) - \ln \left(\sum_{j=1, j \neq n}^{P/2} \varphi_{ajn} \alpha_{1,j} + \sum_{j=1}^{P/2} \varphi_{cjn} \alpha_{2,j} + \sigma_n^2 \right) \\ - \ln \left(\sum_{j=1, j \neq n}^{P/2} \varphi_{bjn} \alpha_{2,j} + \sigma_n^2 \right) + \ln \left(\varphi_{an} \alpha_{1,n} + \sum_{j=1, j \neq n}^{P/2} \varphi_{ajn} \alpha_{1,j} + \sum_{j=1}^{P/2} \varphi_{an} \alpha_{2,j} + \sigma_n^2 \right), \quad (64)$$

where $\varphi_{an} = |\mathbf{z}_{1,n} \cdot \mathbf{h}_{1,n}|^2$, $\varphi_{bn} = |\mathbf{z}_{2,n} \cdot \mathbf{h}_{2,n}|^2$, $\varphi_{cn} = |\mathbf{z}_{1,n} \cdot \mathbf{h}_{2,n}|^2$ and $\varphi_{cjn} = |\mathbf{z}_{1,n} \cdot \mathbf{h}_{2,j}|^2$.

$$R_{sum} = \frac{1}{\ln 2} \sum_m W_{sb} \left[\ln \left(\sum_{j=1, j \neq n}^{P/2} \varphi_{bjn} \alpha_{2,j} + \sigma_n^2 + \varphi_{bn} \alpha_{2,n} \right) + \ln \left(\varphi_{an} \alpha_{1,n} + \sum_{j=1, j \neq n}^{P/2} \varphi_{ajn} \alpha_{1,j} + \sum_{j=1}^{P/2} \varphi_{cjn} \alpha_{2,j} + \sigma_n^2 \right) \right. \\ \left. - \ln \left(\sum_{j=1, j \neq n}^{P/2} \varphi_{ajn} \alpha_{1,j} + \sum_{j=1}^{P/2} \varphi_{cjn} \alpha_{2,j} + \sigma_n^2 \right) - \ln \left(\sum_{j=1, j \neq n}^{P/2} \varphi_{bjn} \alpha_{2,j} + \sigma_n^2 \right) \right], \quad (65)$$

To prove Lemma 1, we need to find the Hessian matrix of (64). For this, take the second derivative with respect to $\alpha_{1,n}$ and $\alpha_{2,n}$.

$$\partial R_{rr} / \partial \alpha_{1,n}^2 = \frac{-\varphi_{an}^2}{(\varphi_{an} \alpha_{1,n} + \sum_{j=1, j \neq n}^{P/2} \varphi_{ajn} \alpha_{1,j} + \sum_{j=1}^{P/2} \varphi_{cjn} \alpha_{2,j} + \sigma_n^2)^2} \quad (66)$$

$$\partial R_{rr} / \partial \alpha_{2,n}^2 = \frac{-\varphi_{cn}^2}{(\varphi_{an} \alpha_{1,n} + \sum_{j=1, j \neq n}^{P/2} \varphi_{ajn} \alpha_{1,j} + \sum_{j=1}^{P/2} \varphi_{cjn} \alpha_{2,j} + \sigma_n^2)^2} + \frac{\varphi_{cn}^2}{(\sum_{j=1, j \neq n}^{P/2} \varphi_{ajn} \alpha_{1,j} + \sum_{j=1}^{P/2} \varphi_{cjn} \alpha_{2,j} + \sigma_n^2)^2} \\ - \frac{\varphi_{bn}^2}{(\sum_{j=1, j \neq n}^{P/2} \varphi_{bjn} \alpha_{2,j} + \sigma_n^2 + \varphi_{bn} \alpha_{2,n})^2} \quad (67)$$

$$\partial R_{rr} / \partial \alpha_{1,n} \partial \alpha_{2,n} = \frac{-\varphi_{an} \varphi_{cn}}{(\varphi_{an} \alpha_{1,n} + \sum_{j=1, j \neq n}^{P/2} \varphi_{ajn} \alpha_{1,j} + \sum_{j=1}^{P/2} \varphi_{cjn} \alpha_{2,j} + \sigma_n^2)^2} \quad (68)$$

As the Hessian matrix is negative semi-definite, because for any vector the answer will always be ≤ 0 , which implies that it is concave in nature. This has been proved by following the arguments similar to the one made in [15].

REFERENCES

1. I. Chih-Lin, C. Rowell, S. Han, Z. Xu, G. Li, and Z. Pan, "Toward green and soft: A 5G perspective," *IEEE Commun. Mag.*, vol. 52, no. 2, pp.6673, 2014.
2. J. Thompson, X.-L. Ge, H.-C. Wu, R. Irmer, H. Jiang, G. Fettweis, and S. Alamouti, "5G wireless communication systems: Prospects and challenges," *IEEE Commun. Mag.*, vol. 52, no. 2, pp.6264, 2014.
3. P. Wang, J. Xiao, and L. Ping, "Comparison of orthogonal and non orthogonal approaches to future wireless cellular systems," *IEEE Veh. Technol. Mag.*, vol. 1, no. 3, pp.411, 2006.
4. Y. Saito, Y. Kishiyama, A. Benjebbour, T. Nakamura, A. Li, and K. Higuchi, "Non-orthogonal multiple access (NOMA) for cellular future radio access," *77th IEEE Veh. Technol. Conf. (VTC Spring)*, 2013.
5. Z. Ding, F. Adachi, and H. V. Poor, "The application of MIMO to non-orthogonal multiple access," *IEEE Trans. Wireless Commun.*, vol. 15, no. 1, pp.537-552, 2016.
6. Z. Ding, Z. Yang, P. Fan, and H. V. Poor, "On the performance of non-orthogonal multiple access in 5G systems with randomly deployed users," *IEEE Signal Process. Lett.*, vol. 21, no. 12, pp.1501-1505, 2014.
7. M. R. Hojiej, J. Farah, C. Nour, and C. Douillar, "Resource allocation in downlink non-orthogonal multiple access (NOMA) for future radio access," *81st IEEE Veh. Technol. Conf. (VTC Spring)*, pp.16, 2015.
8. J. Choi, "Minimum power multicast beamforming with superposition coding for multiresolution broadcast and application to NOMA systems," *IEEE Trans. Commun.*, vol. 63, no. 3, pp. 791800, Mar. 2015.
9. Q. Sun, S. Han, C. L. I, and Z. Pan, "On the ergodic capacity of MIMO NOMA systems," *IEEE Wireless Commun. Letters*, vol. 4, no. 4, pp. 405408, Aug. 2015.
10. E. Larsson, O. Edfors, F. Tufvesson, and T. Marzetta, "Massive MIMO for next generation wireless systems," *IEEE Commun. Mag.*, vol. 52, no. 2, pp. 186195, Feb. 2014.
11. K.Higuchi, Y.Kishiyama, "Non-orthogonal access with random beamforming and intra-beam SIC for cellular MIMO downlink," *IEEE 78th Veh. Technol. Conf. (VTC Fall)*, 2013.
12. Y. Liu, M. ElKashlan, Z. Ding and G.K. Karagiannidis, "Fairness of user clustering in MIMO non-orthogonal multiple access systems," *IEEE Commun. Lett.*, vol. 20, no. 7, pp.1465-1468, 2016.
13. K. Higuchi and Y. Kishiyama, "Non-Orthogonal Access with Random Beamforming and Intra-Beam SIC for Cellular MIMO Downlink," *Proc. IEEE Veh. Technol. Conf. (VTC Fall)*, pp. 15, Sept. 2013.
14. M. F. Hanif, Z. Ding, T. Ratnarajah, and G. K. Karagiannidis, "A minorization-maximization method for optimizing sum rate in the downlink of non-orthogonal multiple access systems," *IEEE Trans. Signal Process.*, vol. 64, no. 1, pp. 7688, Jan. 2016.
15. J.Choi, "On the power allocation for MIMO-NOMA systems with layered transmissions," *IEEE Trans. Wireless Commun.*, vol. 15, no. 5, pp.3226-3237, 2016.
16. Z. Ding, R. Schober, and H. V. Poor, "On the design of MIMO-NOMA downlink and uplink transmission," in *Proc. IEEE Int. Conf. Commun., Kuala Lumpur, Malaysia*, Jun. 2016, to appear.
17. S.Qi, S.Han, I.Chin-Lin, and Z.Pan, "On the ergodic capacity of MIMO NOMA systems," *IEEE Wireless Commun. Lett.*, vol. 4, no. 4, pp.405-408, 2015.
18. L. Dai, B. Wang, Y. Yuan, S. Han, C.-L. I, and Z. Wang, "Non orthogonal multiple access for 5G: Solutions, challenges, opportunities, and future research trends," *IEEE Commun. Mag.*, vol. 53, no. 9, pp. 7481, Sep. 2015.
19. Fei Liu, Petri Mhnen, and Marina Petrova, "Proportional fairness-based user pairing and power allocation for non-orthogonal multiple access," *IEEE 26th Annual International Symposium on Personal, Indoor, and Mobile Radio Communications (PIMRC)*, 2015.
20. Boya Di, Lingyang Song, and Yonghui Li, "Sub-channel assignment, power allocation, and user scheduling for non-orthogonal multiple access networks," *IEEE Tran. Wireless Commun.*, Nov. 2016.
21. B. Kim, W.Chung, S.Lim, S.Suh, J.Kwun, S.Choi, and D.Hong, "Uplink NOMA with multi-antenna," *81st IEEE Veh. Technol. Conf. (VTC Spring)*, pp.15, 2015.
22. Z.Ding, P.Fan, and V.Poor, "Impact of user pairing on 5G non-orthogonal multiple access downlink transmissions," *IEEE Trans. Veh. Technol.*, vol. 65, no. 8, pp. 6010-6023, 2016.
23. M.Al-Imari, P.Xiao, M.A.Imran, and R.Tafazolli, "Uplink non-orthogonal multiple access for 5G wireless networks," *11th Int. Symposium on Wireless Commun. Sys., (ISWCS)*, pp.781-785, 2014.

24. S. Qureshi, S. A. Hassan, "MIMO uplink NOMA with successive bandwidth division," *IEEE Wireless Commun. Networking. Conf. (WCNC Workshops)*, pp.481486, 2016.
25. B. Wang, D. Wang, Linglong, Zhang, Yuan, Mir, Talha and J Li, "Dynamic compressive sensing-based multi-user detection for uplink grant-free NOMA," *IEEE Commun. Lett.*, vol. 20, no. 11, pp. 2320-2323, 2016.
26. S.Chen, K.Peng, and H.Jin, "A suboptimal scheme for uplink NOMA in 5G systems," *IEEE Int. Wireless Commun. and Mobile Computing Conf. (IWCMC)*, pp.1429-1434, 2015.
27. Y. Endo, Y. Kishiyama, and K. Higuchi, "Uplink Non-orthogonal Access with MMSE-SIC in the Presence of Inter-cell Interference, in *Proc. IEEE ISWCS*, 2012.
28. C. W. Sung and Y. Fu, "A game-theoretic analysis of uplink power control for a non-orthogonal multiple access system with two interfering cells, in *Proc. IEEE VTC Spring*, 2016.
29. T. Takeda and K. Higuchi, "Enhanced user fairness using non-orthogonal access with SIC in cellular uplink, in *Proc. IEEE VTC*, Sep. Fall 2011.
30. Y. Endo, Y. Kishiyama, and K. Higuchi, "Uplink Non-orthogonal Access with MMSE-SIC in the Presence of Inter-cell Interference, in *Proc. IEEE ISWCS*, 2012.
31. C. W. Sung and Y. Fu, "A game-theoretic analysis of uplink power control for a non-orthogonal multiple access system with two interfering cells, in *Proc. IEEE VTC*, Spring, 2016.
32. W. Shin, Vaezi, Mojtaba, B. Lee, Love, J. David, J. Lee, and H.V. Poor, "Non-Orthogonal multiple access in multi-cell networks: Theory, performance, and practical challenges," *arXiv:1611.01607*, 2016.
33. Y. Fu, Salaün, Lou, Sung, C. W. Sung, C. S. Chung and M. Coupechoux, "Double iterative waterfilling for sum rate maximization in multicarrier NOMA systems", *IEEE Int. Conf. on Commun. (ICC)*, 2017.
34. L. Lei, D. Yuan, C. K. Ho, and S. Sun, "Joint optimization of power and channel allocation with non-orthogonal multiple access for 5G cellular systems, in *Proc. IEEE Global Commun. Conf.*, pp. 1-6, Dec. 2014.
35. Z.Ding, M.Peng, and H.V.Poor, "Cooperative non-orthogonal multiple access in 5G systems," *IEEE Commun. Lett.*, vol. 19, no. 8, pp.14621465, 2015.
36. S. A. R. Naqvi, S. A. Hassan, "Combining NOMA and mmWave technology for cellular communication," *IEEE Veh. Technol. Conf. (VTC Fall)*, Sep 2016.
37. Y. Saito, A. Benjebbour, Y. Kishiyama, and T. Nakamura, "System-level performance evaluation of downlink non-orthogonal multiple access (NOMA)," *PIMRC*, pp.611615, 2013.
38. Z. Q. Al-Abbasi and D. K. C. So, "Power allocation for sum rate maximization in non-orthogonal multiple access system," *IEEE 26th Annual International Symposium on Personal, Indoor, and Mobile Radio Communications (PIMRC)*, pp.16491653, 2015.
39. P. Parida and S. S. Das, "Power allocation in OFDM based NOMA systems: A DC programming approach," *IEEE Global Telecommun. Conf. (GLOBE-COM Workshops)*, 2014.
40. N. Otao, Y. Kishiyama, and K. Higuchi, "Performance of non-orthogonal multiple access with SIC in cellular downlink using proportional fair-based resource allocation," *IEICE Trans Commun.*, vol. 98, no. 2, pp.344351, 2015.
41. M. Al-Imari, P. Xiao, and M. Ali Imran, "Receiver and resource allocation optimization for uplink NOMA in 5G wireless network, *IEEE International Symposium on Wireless Communication Systems (ISWCS)*, pp. 151155, 2015.
42. H. Tabassum, M. S. Ali, E. Hossain, M. J. Hossain, and D.-I. Kim, "Non-orthogonal multiple access (NOMA) in cellular uplink and downlink: Challenges and enabling techniques, *arXiv:1608.05783*, 2016.
43. W. Yu, W. Rhee, S. Boyd, and J. Cioffi, "Iterative water-filling for gaussian vector multiple-access channels, *IEEE Trans.Inf. Theory*, vol. 50, no. 1, pp. 145152, Jan. 2004.

AUTHORS' BIOGRAPHIES

Soma Qureshi received her BS degree in Electronics Engineering from University of Engineering and Technology, Taxila, Pakistan, in 2014. Currently, she is pursuing her MS degree in Electrical Engineering from National University of Sciences and Technology (NUST), Pakistan.

Syed Ali Hassan received his PhD in Electrical Engineering from Georgia Institute of Technology, Atlanta

USA in 2011. He received his MS Mathematics from Georgia Tech in 2011 and MS Electrical Engineering from University of Stuttgart, Germany in 2007. He was awarded BE degree in Electrical Engineering from National University of Sciences and Technology (NUST), Pakistan, in 2004. His broader area of research includes signal processing, stochastic modeling, estimation and detection theory, and smart grid communications.

Dushantha Nalin K. Jayakody received the Ph. D. degree in Electronics, Electrical and Communications Engineering in 2014, from the University College Dublin, Ireland. He received his MSc degree in Electronics and Communications Engineering from the Department of Electrical and Electronics Engineering, Eastern Mediterranean University, Turkey in 2010 (under the University full graduate scholarship) and ranked as the first merit position holder of the department, and B. E. electronics engineering degree (with first-class honors) from Pakistan in 2009 and was ranked as the merit position holder of the University (under PTAP Scholarship.). From 2014 - 2016, he was a Postdoc Research Fellow at the Institute of computer science, University of Tartu, Estonia and Department of Informatics, University of Bergen, Norway. From summer 2016, he is Professor at the Department of Software Engineering, Institute of Cybernetics, National Research Tomsk Polytechnic University, Russia where he also serves as the Director of Tomsk Infocomm Lab. Dr. Jayakody is a Member of IEEE and he has served as session chair or technical program committee member for various international conferences, such as IEEE PIMRC 2013/2014, IEEE WCNC 2014/2016, IEEE VTC 2015 etc. He currently serve as a lead guest editor for Elsevier Physical Communications Journal.